

# Vascular Cell Adhesion Molecule-1 Is a Regulator of Ovarian Cancer Peritoneal Metastasis

Jill K. Slack-Davis,<sup>1,4</sup> Kristen A. Atkins,<sup>2,4</sup> Christine Harrer,<sup>1</sup> E. Daniel Hershey,<sup>1</sup> and Mark Conaway<sup>3,4</sup>

Departments of <sup>1</sup>Microbiology, <sup>2</sup>Pathology, and <sup>3</sup>Health Evaluation Sciences and <sup>4</sup>Cancer Center, University of Virginia, Charlottesville, Virginia

## Abstract

**Ovarian cancers metastasize by attaching to and invading through the mesothelium, a single layer of mesothelial cells lining the peritoneal cavity. The presence of invasive peritoneal metastases is associated with a poor prognosis for ovarian cancer (5-year survival <25%). Vascular cell adhesion molecule-1 (VCAM-1) is a cell surface receptor that mediates leukocyte attachment and extravasation across endothelial and mesothelial monolayers at sites of inflammation. Membranous VCAM-1 expression was observed on the mesothelium of 13 of 14 women with ovarian cancer compared with 6 of 15 who were cancer-free. Using a cell culture model system of mesothelial invasion, highly tumorigenic SKOV-3 and ES-2 cells were 2.5 to 3 times more efficient in transmigration through the mesothelial monolayer compared with poorly tumorigenic OVCAR-3 cells. Blocking antibodies to, or small interfering RNA knockdown of, VCAM-1 or its ligand  $\alpha_4\beta_1$  integrin significantly decreased, but did not completely inhibit, transmigration of SKOV-3 cells through mesothelial monolayers. Furthermore, using a mouse model of ovarian cancer metastasis, treatment with VCAM-1 function-blocking antibodies decreased tumor burden and increased survival. Together, these observations implicate VCAM-1- $\alpha_4\beta_1$  integrin interactions in the regulation of ovarian cancer cell mesothelial invasion and metastatic progression and offer the possibility of novel therapeutic targets. [Cancer Res 2009;69(4):1469–76]**

## Introduction

Ovarian cancer is the deadliest of the gynecologic malignancies. Approximately 22,000 new cases of ovarian cancer are diagnosed and 15,000 deaths occur each year (1). The relatively poor prognosis for ovarian cancer is due largely to the advanced stage of disease at the time of diagnosis (2). Approximately 75% of patients are diagnosed with stage III or IV ovarian cancer, which is characterized by peritoneal or distant metastases, respectively, and is accompanied by a 5-year survival of 25%. Although the majority of patients with metastatic ovarian cancer initially respond well to surgical resection and chemotherapy, 50% to 75% of these patients will have recurrent disease (3).

Ovarian cancer metastasis is a complex process involving many different routes. Unlike most solid tumors, ovarian cancer metastasizes initially by spreading throughout the peritoneal cavity,

where it preferentially attaches to and invades through the mesothelium, a layer of mesothelial cells that lines the peritoneum and surrounds the serosal surface of organs in these cavities (e.g., colon and liver). The ability of ovarian cancer cells to invade through the mesothelium is associated with a poor prognosis (4). Although hematogenous spread to the liver or lungs is observed, it is relatively uncommon; 15% of patients are diagnosed with stage IV disease. Women diagnosed with peritoneal metastasis (stage III) typically recur as stage III and succumb to complications arising from excessive abdominal tumor bulk. The presence of microscopic liver or lung lesions in this patient population has not been evaluated. The mechanisms that regulate ovarian cancer metastasis are poorly understood. It is believed that ovarian cancer is uniquely positioned to metastasize to the peritoneum due to its surface growth and proximity to the peritoneal cavity. Although the importance of location cannot be denied, it is also likely that the peritoneal microenvironment favors implantation of ovarian cancer cells on the peritoneal lining.

The mesothelium secretes proinflammatory cytokines, growth factors, and extracellular matrix components (5, 6). In particular, conditioned medium from mesothelial cell cultures was found to contain lysophosphatidic acid (LPA) and fibronectin, both of which stimulated ovarian cancer cell migration (5, 6). Moreover, LPA is a principal component of ascites that accumulates in ovarian cancer patients (7). Adhesion of the migrating cells to the mesothelium is mediated in part by  $\beta_1$  integrins expressed on ovarian cancer cells (8). Ovarian cancer metastasis was proposed to be regulated by  $\beta_1$  integrin binding to fibronectin secreted by mesothelial cells (8). The interaction with fibronectin would serve to anchor the cancer cells; however, it does not explain their ability to pass between mesothelial cells (9), a process that, similar to leukocyte extravasation, likely involves active participation between mesothelial and ovarian cancer cells. More recently, increased adhesion receptor [in particular, vascular cell adhesion molecule-1 (VCAM-1)] and cytokine gene expression have been reported within the peritoneal lining and underlying stroma of ovarian cancer patients compared with the peritoneum of patients with benign gynecologic conditions (10). Together, these observations implicate active participation and communication between cancer cells and the mesothelium in the regulation of metastasis.

VCAM-1 is a cell surface receptor expressed on activated endothelial and mesothelial cells, which functions to regulate leukocyte attachment and extravasation at sites of inflammation (11, 12). Inflammatory cytokines and leukocyte attachment increase endothelial expression of VCAM-1, activate signaling cascades, and result in endothelial retraction and passage of leukocytes through the endothelial barrier. VCAM-1 binds  $\alpha_4\beta_1$  integrins expressed on leukocytes to promote extravasation. Additionally,  $\alpha_4\beta_1$  integrin expression has been shown on a variety of cancers (13–17). Moreover, treating melanoma cells with  $\alpha_4\beta_1$  integrin function-blocking antibodies prevented extravasation and lung metastasis following

**Note:** Supplementary data for this article are available at Cancer Research Online (<http://cancerres.aacrjournals.org/>).

**Requests for reprints:** Jill K. Slack-Davis, Department of Microbiology, University of Virginia, P. O. Box 800734, Charlottesville, VA 22908. Phone: 434-924-5341; Fax: 434-982-0689; E-mail: jks6a@virginia.edu.

©2009 American Association for Cancer Research.  
doi:10.1158/0008-5472.CAN-08-2678

tail vein injection in a mouse model (18, 19), thus implicating VCAM-1- $\alpha_4\beta_1$  integrin interactions in metastatic progression.

We investigated the role of VCAM-1 in the regulation of one aspect of ovarian cancer metastasis: mesothelial invasion. VCAM-1 protein was found to be preferentially expressed on the mesothelium of ovarian cancer patients compared with the mesothelium of women without cancer. Ovarian cancer cell invasion of the mesothelium was quantified using a coculture assay system. Inhibition of VCAM-1 function in the coculture system decreased ovarian cancer transmigration of the mesothelium. Lastly, treatment of mice in an ovarian cancer metastasis model with VCAM-1 function-blocking antibodies decreased tumor burden and increased survival. Together, these findings implicate VCAM-1- $\alpha_4\beta_1$  integrin interactions in the regulation of mesothelial cell transmigration and ovarian cancer metastatic invasion.

## Materials and Methods

**Reagents.** The following antibodies were used (Millipore unless otherwise indicated):  $\alpha_4$  integrin (clone HP2/1),  $\alpha_5$  integrin (clone SAM-1),  $\alpha_6\beta_1$  integrin (clone Y9A2),  $\beta_1$  integrin (clone P2D2), VCAM-1 (clone IE5 or P3C4), mouse IgG1 (clone DD7), mouse IgG2b (clone DD311), Fc $\gamma$ III/II receptor (Mouse BD Fc Block; BD Biosciences), anti-human VCAM-1 (clone 1.4C3; Novocastra Laboratories), and anti-mouse VCAM-1 (H-276; Santa Cruz Biotechnology) for immunohistochemistry and rat anti-mouse VCAM-1 hybridoma clone M/K-2.7 originated by Dr. P. Kincade (21) and provided by Dr. Klaus Ley (University of Virginia) for animal studies.

**Cell lines.** SKOV-3 [American Type Culture Collection (ATCC)] and ES-2 cells (gift of Dr. A. Jazaeri, University of Virginia) were grown in McCoy's 5A medium supplemented with 10% fetal bovine serum (FBS); OVCAR-3 cells (ATCC) in RPMI 1640, 10% FBS; and CaOV-3 and IGROV cells (gift of Dr. A. Jazaeri) in RPMI 1640, 10% FBS, 0.75% sodium bicarbonate (w/v), and 2 mmol/L sodium pyruvate. SKOV3ip1 cells, a variant of SKOV-3 passaged once through the peritoneum to improve tumor take, were provided by Dr. A. Sood (M. D. Anderson Cancer Center, Houston, TX), grown in RPMI 1640, 15% FBS, and used for the animal studies. LP9 mesothelial cells (passage 7–11), a nontransformed primary cell line derived from the ascites of an ovarian cancer patient (Coriell Cell Repository, Camden, NJ), were grown in 1:1 M199:MCDB110, 2 mmol/L L-glutamine, 15% FBS, 10 ng/mL epidermal growth factor, and 0.4  $\mu$ g/mL hydrocortisone.

**Human tissue samples and immunohistochemistry.** Deidentified human tissue and fluid samples were obtained and used in accordance with the University of Virginia Human Investigation Committee guidelines. Paraffin-embedded peritoneal or omentum biopsies devoid of malignancy or cell pellets of peritoneal washings or ascites from women diagnosed with ovarian cancer or those who were cancer-free were obtained from the surgical pathology archives. Sections (5  $\mu$ m) were boiled in 1 mmol/L EDTA (pH 8.0) and stained with anti-human VCAM-1 antibody followed by horseradish peroxidase-conjugated secondary antibody. VCAM-1 staining was evaluated blinded to the original patient diagnosis. The percentage of mesothelial cells expressing membranous VCAM-1 was documented >50%. Fisher's exact test assessed significance of VCAM-1 expression in cancer versus cancer-free patient samples.

**Transmesothelial migration assay.** LP9 mesothelial cells were plated on glass coverslips for 24 h, labeled with CellTracker Orange (Invitrogen), and allowed to grow to confluence (48 h from time of plating). Monolayer integrity was determined using a cell permeability assay, which was developed for endothelial monolayers and measures the movement of molecules between cells of the monolayer (22). Briefly, monolayers were grown on 3- $\mu$ m pore filters in Fluoroblok chambers (BD Falcon) and incubated with 1 mg/mL FITC-dextran (70 kDa; Sigma) for 30 min at 37°C, and fluorescence in the bottom chamber was read using Synergy 2 plate reader (BioTek) and Gen5 software (BioTek). Ovarian cancer cells (10<sup>5</sup>) labeled with CellTracker Green (Invitrogen) were seeded on mesothelial monolayers. Six hours after seeding, cell cultures were fixed with 4% para-

formaldehyde in PBS for 15 min at room temperature and mounted. Confocal microscopy was used to obtain 1- $\mu$ m Z-stacks using a custom-modified Nikon Eclipse TE2000 confocal microscope. An image within the top third of the stack was obtained, and green cells were false-colored blue and merged with an image from the bottom third of the stack. The ratio of nonoverlapping green cells to total cells in the field represents the percent of cells migrating through the monolayer (Fig. 2A). For antibody blocking studies, SKOV-3 cells and LP9 monolayers were treated with 10  $\mu$ g/mL receptor-blocking antibody or IgG isotype control for 30 min before plating SKOV-3 cells onto monolayers in the continued presence of blocking antibody. At least 50 cells in three or more experiments were scored. The data represent the mean  $\pm$  SE. Each experimental group was analyzed using single-factor ANOVA. If the global *F* test for differences among any one of the groups was significant at the 5% level, the Tukey's post test was used to investigate which treated group(s) differed from controls. Statistical significance was defined as *P* < 0.05.

**Small interfering RNA transfections.** RNA interference (RNAi) oligomers were obtained from Dharmacon for human VCAM-1 (SMART-pool) and human  $\alpha_4$  integrin (23). siGLO RISC-Free small interfering RNA (siRNA; Dharmacon) served as negative control. LP9 cells (10<sup>6</sup>) were transfected with 2  $\mu$ g VCAM-1 RNAi oligomer using Nucleofector Basic Endothelial Solution and Program T-23 (Amaxa); SKOV-3 cells (10<sup>6</sup>) were transfected with 2  $\mu$ g  $\alpha_4$  integrin RNAi oligomer using Nucleofector Solution V and Program V-05.

**Flow cytometry.** Integrin and VCAM-1 antibodies labeled with phycoerythrin using the Zenon labeling kit (Invitrogen) were incubated with 10<sup>6</sup> ovarian cancer or mesothelial cells at 4°C for 30 min. Following three PBS washes, antibody-bound cells were examined using a FACSCalibur cytometer (BD Biosciences); data were analyzed using FlowJo software version 8.5.2 for Macintosh (Tree Star).

**Animal studies.** Female athymic nude mice (NCR-nu) purchased from the National Cancer Institute-Frederick Cancer Research and Development Center or Taconic Farms, Inc. were injected i.p. with 10<sup>6</sup> SKOV3ip1 cells at 8 to 12 wk of age and monitored daily for signs of distress, including weekly weighing, observation of activity and skin appearance, and obtaining weekly whole-blood cell counts. Mice were euthanized 2, 4, or 6 wk after tumor initiation or if showing signs of distress, and the mice were weighed, ascites volume was measured, the number and location of macroscopic lesions were recorded, and tumor-containing tissues including the omentum, reproductive tract, liver, and lung were collected and fixed in formalin. Tissues were embedded in paraffin, sectioned, and stained with H&E. The number of microscopic nodules was counted and the extent of invasion was scored.

Blocking VCAM-1 function on tumor growth and survival was tested by injecting 200  $\mu$ g anti-VCAM-1 function-blocking antibody (21) together with the tumor cells i.p. and twice weekly thereafter, a treatment course that was determined to maintain elevated serum antibody titers (data not shown). Rat anti-mouse IgG (Anogen) served as the negative control. Mice were euthanized 4 and 6 wk after tumor initiation or if moribund and evaluated for the extent of tumor formation as described above. The number of days to moribund was recorded for survival analysis. The experiment was terminated once the median survival for treated and control groups was obtained and the treated animals were within a week of twice the age of the median survival of the control group.

## Results

**Peritoneal VCAM-1 expression in ovarian cancer patients.** VCAM-1 gene expression has been reported within the mesothelium of microdissected peritoneal biopsies of women with ovarian cancer (10). To determine if mesothelial cells expressed VCAM-1 protein, immunohistochemistry was performed on peritoneal biopsies or cell blocks made from pelvic washings from individuals with or without ovarian cancer (Fig. 1). In tissue sections devoid of ovarian cancer, mesothelial cells were visible outlining the omentum or peritoneum (Fig. 1, *arrows*), and these cells stained

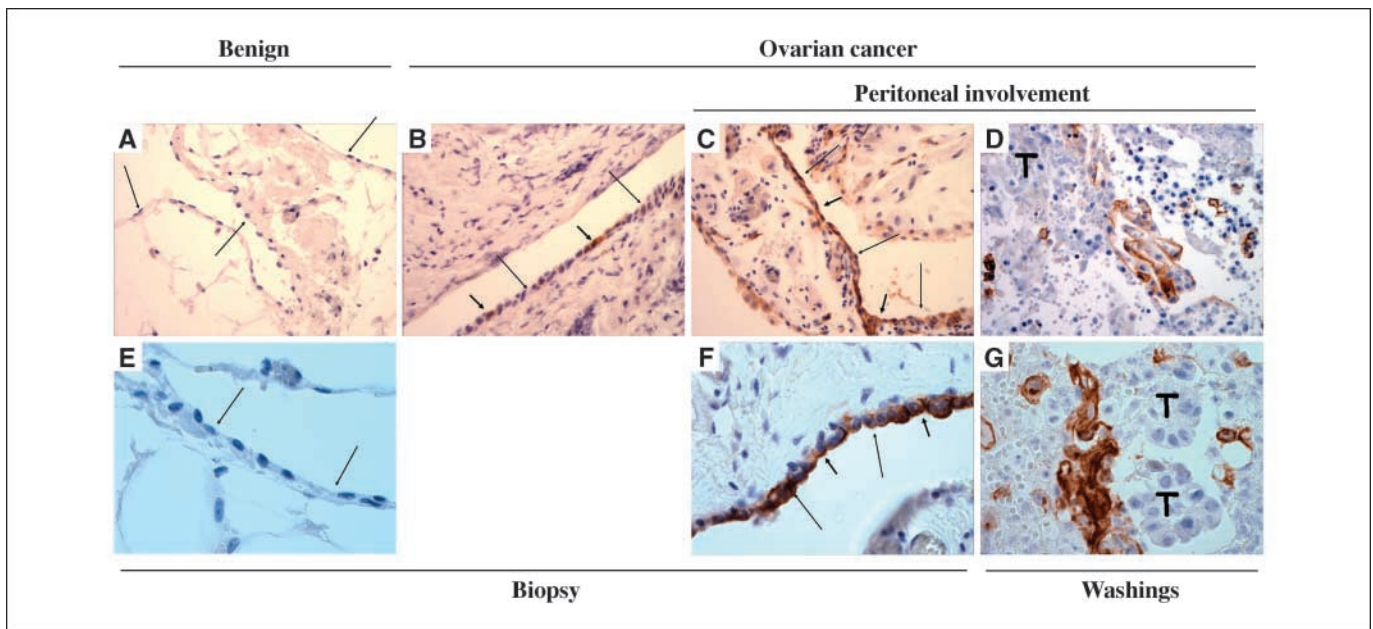


**Figure 1.** Mesothelial VCAM-1 expression. Immunohistochemistry was used to detect VCAM-1 expression (arrowhead) on the mesothelium (arrow) of peritoneal biopsies (A, B, C, E, and F) or cells in peritoneal washings (D and G) from women with benign conditions (A and E) or ovarian cancer (B, C, D, F, and G). Tissue biopsies were devoid of tumor; peritoneal washings contained tumor, mesothelial, and immune cells. Original magnification,  $\times 100$  (A–D) and  $\times 400$  (E–G).

positively for VCAM-1 in biopsies obtained from cancer patients (Fig. 1B, C, and F, arrowheads). VCAM-1 expression was also observed on mesothelial cells present in samples from pelvic washings (Fig. 1D and G). Mesothelial cells examined from biopsies or washings from 13 of 14 ovarian cancer patients were positive for VCAM-1 expression. Ten of the 13 VCAM-1-expressing samples had  $>50\%$  of cells staining positively. In patients with advanced-stage ovarian cancer (i.e., stage III or IV that contain peritoneal metastases), the entire mesothelial cell layer was positive for VCAM-1 expression (Fig. 1C and F, arrowhead) compared with those cases without peritoneal involvement (i.e., stage I or II)

where VCAM-1 reactivity was localized to discrete patches of mesothelial cells (Fig. 1B, arrowhead). In contrast, significantly fewer peritoneal biopsies or washings from women free of cancer showed VCAM-1 reactivity on the mesothelial cells (6 of 15 samples;  $P = 0.005$ , Fisher's exact test), and only 3 had  $>50\%$  positive cells.

**VCAM-1 and ovarian cancer invasion of the mesothelium.** A cell culture-based assay was developed to quantify the ability of ovarian cancer cells to pass through the mesothelium (hereafter referred to as "transmesothelial migration"). Ovarian cancer cells were plated on LP9 mesothelial monolayers, and transmesothelial

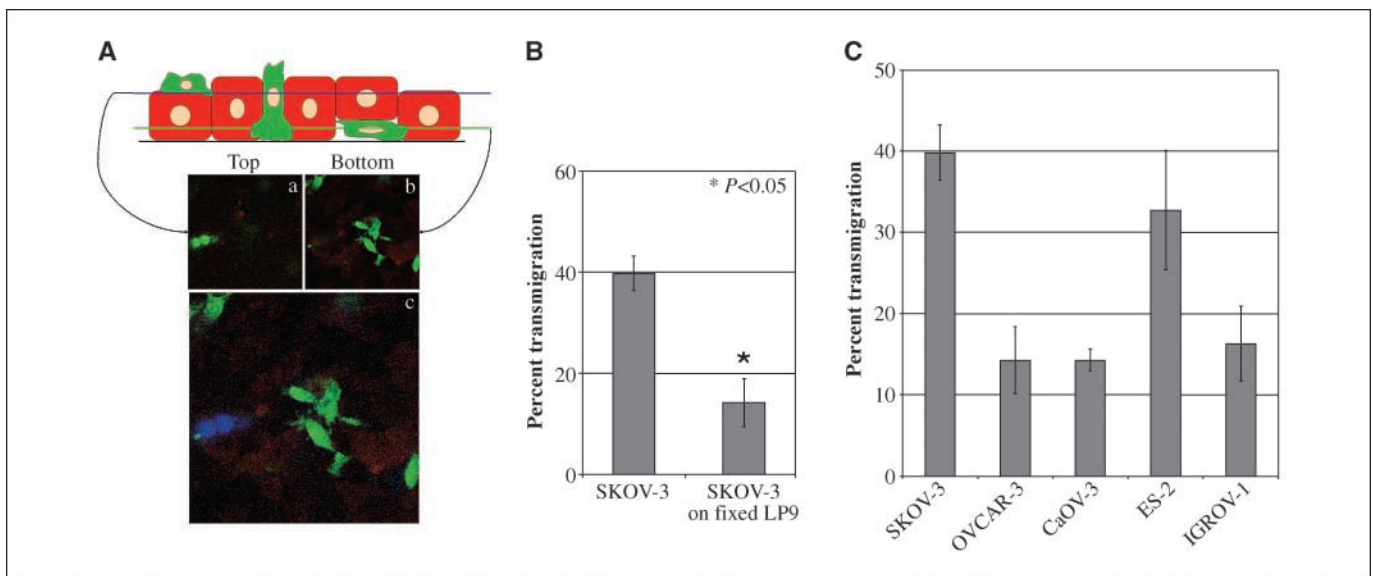


**Figure 2.** Ovarian cancer cell migration through a mesothelial monolayer. A, schematic representation of the methodology used to quantify transmesothelial migration. See text for details. B, confluent mesothelial cells (LP9) were either left viable (left bar) or fixed (right bar). Green SKOV-3 cells were plated on the monolayer for 6 h and fixed and transmesothelial migration was quantified. C, percent transmesothelial migration of various ovarian cancer cell lines.



migration was quantified as described (Materials and Methods; Fig. 2A); permeability assays confirmed the integrity of the monolayer (data not shown). Transmesothelial migration increased over time (data not shown) with maximal levels (40–45%) achieved 6 hours after plating (Fig. 2B). To show that the mesothelial cells actively participated in the transmesothelial migration process, LP9 monolayers were fixed before plating labeled SKOV-3 cells. Only 15% of the SKOV-3 cells were found in the bottom third of the fixed, immobile monolayer (Fig. 2B). Moreover, although treatment of mesothelial monolayers with tumor necrosis factor  $\alpha$  (TNF $\alpha$ ) increased mesothelial monolayer permeability, it had no effect on transmesothelial migration (data not shown). These observations indicate that both the ovarian cancer cells and mesothelial cells participate in the invasion process and that the existence of preformed holes in the monolayer is insufficient to promote transmesothelial migration.

To determine whether this model reflected the metastatic properties of ovarian cancer cells, the transmesothelial migratory capacity for a panel of ovarian cancer cell lines was assessed. SKOV-3 and ES-2 cell lines showed the highest levels of transmesothelial migration (40% and 37%, respectively; Fig. 2C), correlating with their ability to form invasive metastatic tumors in mice. OVCAR-3, CaOV-3, and IGROV1 cells showed 15% to 18% transmesothelial migration, equivalent to the extent of transmesothelial migration through fixed mesothelial monolayers (compare Fig. 2B and C). These observations correlated with the migratory capacity of SKOV-3, ES-2, and OVCAR-3 cells (data not shown) and paralleled the extent of  $\alpha_4$  integrin expression on each line (Supplementary Table), indicating a potential role for  $\alpha_4$  integrin in this process.

Data from human peritoneal biopsy samples indicated a correlation between VCAM-1 expression and the presence of malignant disease (Fig. 1). LP9 mesothelial cells constitutively expressed VCAM-1; ovarian cancer cell lines expressed known ligands for VCAM-1 (i.e.,  $\alpha_4\beta_1$  and  $\alpha_9\beta_1$  integrins; Supplementary Table). The role of VCAM-1 and various integrins in transmesothelial migration was assessed using blocking antibodies to inhibit function and siRNA oligomers to knock down expression. Increasing concentrations of VCAM-1 blocking antibodies resulted in a dose-dependent decrease in transmesothelial migration of SKOV-3 cells (Supplementary Figure). Indeed, cultures treated with control IgG antibodies had two times greater transmesothelial migration compared with cultures treated with anti-VCAM-1,  $\alpha_4$ , or  $\beta_1$  integrin-blocking antibodies (Fig. 3A). Antibody blockade of  $\alpha_5$  or  $\alpha_9\beta_1$  integrin had no effect on transmesothelial migration (Fig. 3A). Treatment of LP9 cells with VCAM-1 siRNA or SKOV-3 cells with siRNA to  $\alpha_4$  or  $\alpha_5$  integrin reduced surface expression of each molecule to <10% the level observed on control cells (Fig. 3B; data not shown). Both VCAM-1 knockdown in LP9 cells or  $\alpha_4$  integrin knockdown in SKOV-3 cells decreased transmesothelial migration, whereas inhibition of  $\alpha_5$  integrin expression had no effect (Fig. 3B; data not shown), thus supporting the blocking antibody data.

**Mouse model of ovarian cancer metastasis.** I.p. injection of human ovarian cancer cells into immune compromised mice has been used as a model for peritoneal metastasis of human ovarian cancer (20, 24). SKOV3ip1 cells were injected into the peritoneum of athymic nude mice. Complete necropsy was performed 2, 4, and 6 weeks after injection to monitor the kinetics and extent of tumor formation. Microscopic, noninvasive tumors were observed on the omentum of mice 2 weeks after injection (Fig. 4A, a). The tumor

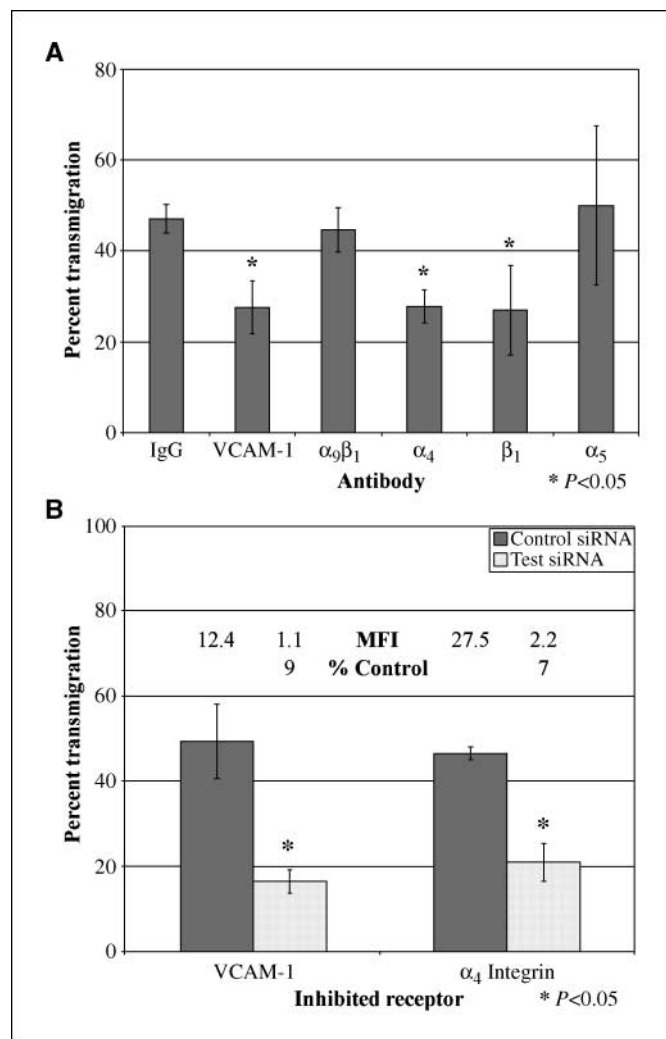


**Figure 3.** VCAM-1 and  $\alpha_4\beta_1$  integrin regulate transmesothelial migration. **A**, transmesothelial migration of SKOV-3 cells with function-blocking antibodies directed against the indicated adhesion receptors or IgG control. **B**, transmesothelial migration of SKOV-3 cells following VCAM-1 knockdown in LP9 mesothelial cells or  $\alpha_4$  integrin knockdown in the cancer cells. Flow cytometry confirmed surface VCAM-1 or  $\alpha_4$  integrin expression. Mean fluorescence intensity (MFI), VCAM-1 or  $\alpha_4$  integrin levels normalized to the isotype control. % Control, MFI of cells treated with the test siRNA relative to control.

nodules were observed on top of the mesothelium, where they exhibited a smooth tumor/mesothelial interface and did not invade into fat or incite a desmoplastic host response. By 4 weeks, macroscopic tumors were visible seeding the omentum and fatty tissue surrounding the reproductive tract. Histologic evaluation of tissues from the peritoneal cavity revealed invasive tumors growing under the mesothelium in the omentum (Fig. 4A, b) and the peritoneal muscle wall (data not shown). Individual tumor cells invading the omentum were observed adjacent to fibroblast-like cells within the tumor, indicative of a "host" response (b, star). A single-cell layer of mesothelial cells was seen surrounding the tumor (b, arrows). There was no evidence of distant metastases 4 weeks after injection. Extensive tumor dissemination throughout the peritoneal cavity in addition to ascites accumulation was observed 6 weeks after injection. Notably, microscopic lesions were observed in the lungs of injected animals (Fig. 4A, c). To determine if the mouse model mimicked human ovarian cancer with regard to peritoneal

VCAM-1 expression, sections of mouse omentum were stained using immunohistochemistry. Mesothelial cells of mice injected with SKOV3ip1 cells stained positively for VCAM-1 (Fig. 4B, *b*, arrows) compared with uninjected controls (*a*). Together, these observations indicate that i.p. injection of human tumor cells into immune compromised mice mimics the peritoneal spread, distant metastasis, and VCAM-1 expression observed in human ovarian cancer.

**VCAM-1 blockade slows ovarian cancer metastasis in the mouse model.** To determine if VCAM-1 played a role in metastatic dissemination of SKOV3ip1 cells in the mouse model, VCAM-1 function-blocking or IgG control antibodies were injected i.p. together with the cells and twice weekly thereafter. Experimental groups were established to monitor survival and assess the extent of disease 4 and 6 weeks after tumor initiation. In the absence of anti-VCAM-1 antibody treatment, median survival was 41 days (range, 32-56 days; Fig. 5A). In contrast, the median survival of anti-VCAM-1-treated mice was 2 weeks longer (56 days; range, 40 to >78; Fig. 5A). The survival experiment was terminated at 78 days with three of seven anti-VCAM-1-treated mice showing no signs of distress. Indeed, two of these mice lacked macroscopic tumor nodules; microscopic lesions were present. The tumor burden in the anti-VCAM-1-treated groups was not statistically different from control (data not shown).

The results of the survival experiment indicate a delay in tumor progression following VCAM-1 blockade. To examine this possibility more carefully, experiments were initiated to evaluate tumor burden 4 and 6 weeks after initiation. Tumor burden was assessed by evaluating (*a*) volume of ascites, (*b*) presence of microscopic lung metastases, and (*c*) the incidence and extent of invasive macroscopic tumor nodules. Six weeks after tumor initiation,

the mean volume of ascites obtained from the control group was 10 times greater than the anti-VCAM-1-treated group ( $6.6 \pm 1.2$  mL versus  $0.6 \pm 0.4$  mL; Fig. 5B). The incidence of microscopic lung metastasis was also reduced by VCAM-1 antibody treatment; 8 of 10 control mice compared with 3 of 10 anti-VCAM-1-treated mice contained lung metastases (Fig. 5C). The incidence of mice with macroscopic peritoneal tumor nodules and the number of nodules per mouse 4 weeks after tumor initiation was reduced following anti-VCAM-1 antibody treatment (Fig. 6A). All 10 of the mice that received control antibodies contained macroscopic peritoneal tumor nodules (Fig. 6A) located primarily on the omentum and in some cases seeding the peritoneal wall, pancreas, and diaphragm (data not shown). In contrast, only five of nine mice treated with anti-VCAM-1 function-blocking antibodies had visible tumor nodules. Moreover, 6 of 10 control mice had >50 nodules within the peritoneum compared with only 1 of the anti-VCAM-1-treated group. These observations indicate that treatment with function-blocking antibodies directed against VCAM-1 reduced metastatic tumor burden in the mouse model.

Because VCAM-1 partially inhibited transmesothelial migration (Fig. 3), the extent of tumor invasion within the peritoneal cavity was examined histologically (Fig. 6B) and classified into three groups. Noninvasive tumors rested on top of the mesothelium with a smooth tumor-mesothelial interface (*a* and *b*). Minimally invasive tumors (+) exhibited a smooth interface for the majority of the border between the mesothelium and tumors; however, they contained small regions of infiltration into the underlying tissue (*c* and *d*). Highly invasive tumors (+++) grew under the mesothelium, typically taking over the entire underlying tissue and eliciting a desmoplastic response (*e*). Within 4 weeks of tumor initiation, the majority of control mice (8 of 10) had highly invasive

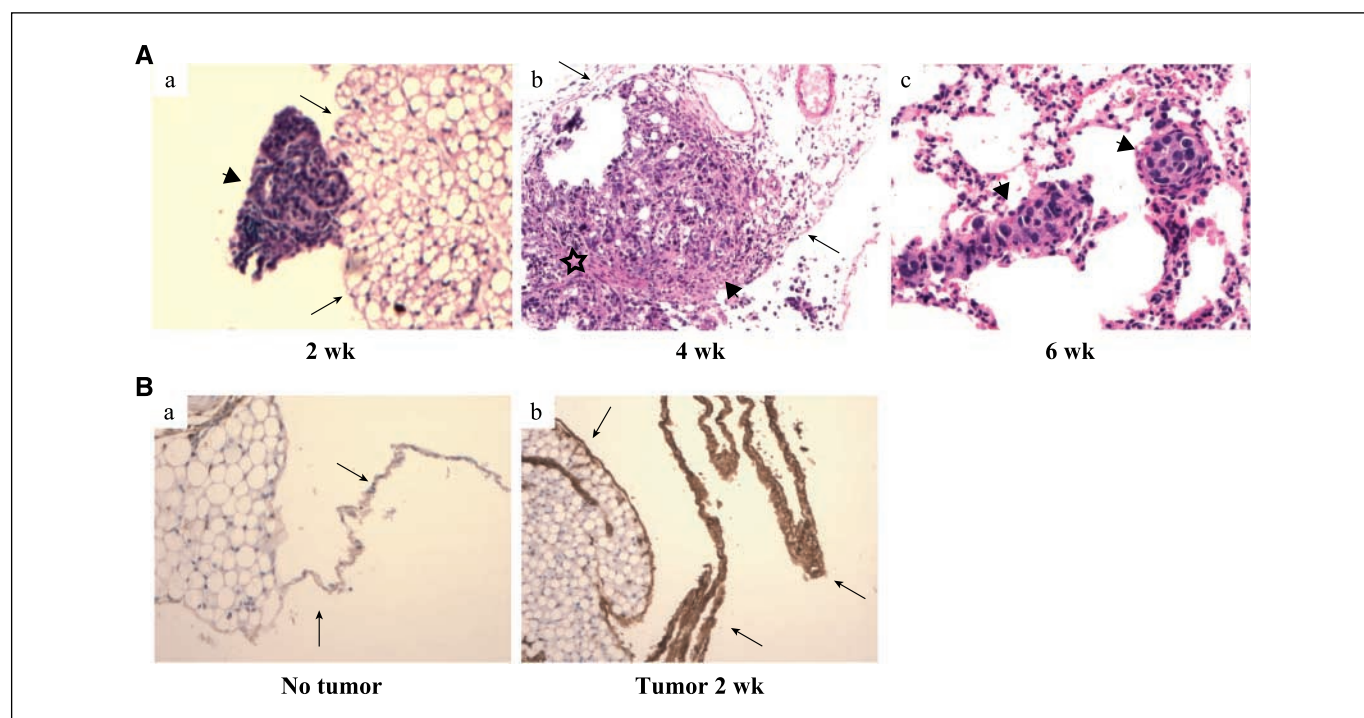


**Figure 4.** Orthotopic model of ovarian cancer metastasis. *A*, tissue specimens (*a* and *b*, omentum; *c*, lung) from mice injected with SKOV3ip1 cells were examined 2 wk (*a*), 4 wk (*b*), and 6 wk (*c*) after injection for the presence of tumor cells following H&E staining. Arrowhead, tumor nodule; arrow, mesothelium; star, desmoplastic host response. Original magnifications,  $\times 100$  (*a* and *b*) and  $\times 200$  (*c*). *B*, VCAM-1 expression was detected by immunohistochemistry on the mesothelium (arrows) of mice receiving tumor cells (*b*) compared with control animals (*a*). Original magnification,  $\times 100$ .

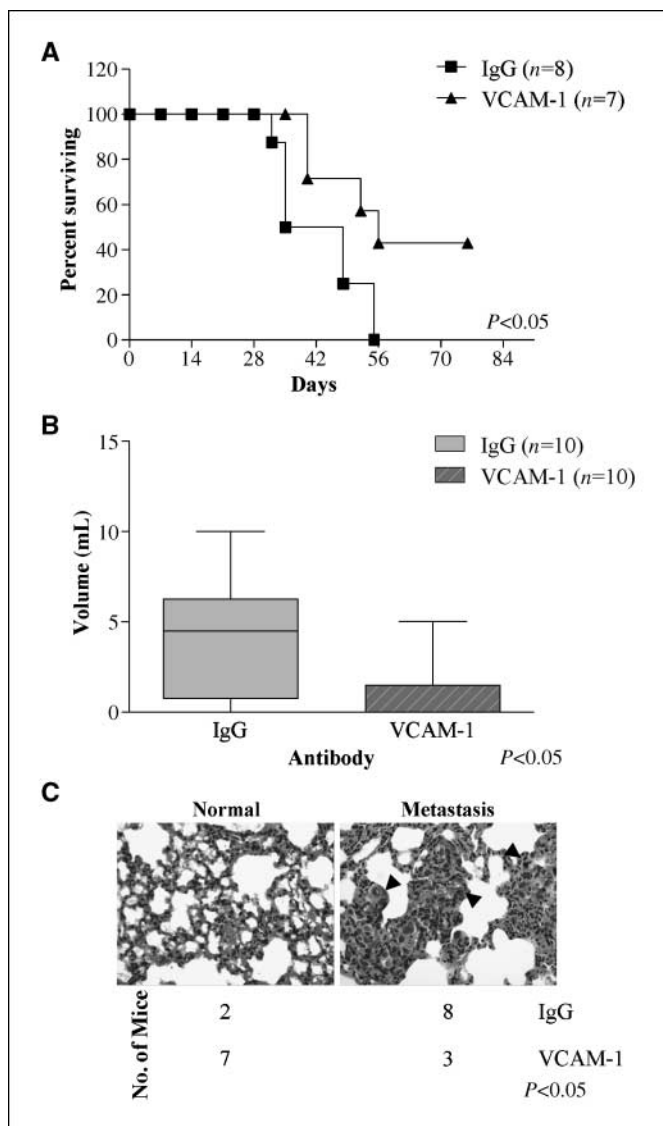


**Figure 5.** Anti-VCAM-1 antibody treatment increased survival in an orthotopic model of ovarian cancer metastasis. **A**, survival analysis of tumor-bearing mice treated with anti-VCAM-1 ( $\blacktriangle$ ) or control IgG ( $\blacksquare$ ) antibody. Log-rank test assessed statistical significance. **B**, 6 wk after tumor initiation, the number of tumor-bearing mice with ascites was scored and the volume was measured. Mann-Whitney statistic assessed significance. **C**, H&E-stained sections of normal mouse lung (**a**) or a lung section containing microscopic tumor nodules (**b**, arrowheads) 6 wk after tumor initiation. Original magnification,  $\times 200$ . The number of mice with lung metastases is indicated. Fisher's exact test assessed significance.

tumors compared with only 2 of 9 anti-VCAM-1-treated mice. Two additional anti-VCAM-1-treated mice had minimally invasive tumors, whereas the majority of mice receiving VCAM-1 antibody treatment either had no evidence of tumors or no mesothelial invasion. Collectively, the animal studies show that treatment with function-blocking antibodies directed against VCAM-1 reduced tumor burden and mesothelial invasion, likely contributing to the observed increase in survival.

## Discussion

The data reported here uncover a role for VCAM-1 in the regulation of ovarian cancer metastatic invasion. VCAM-1 was

expressed preferentially on the mesothelium of women with ovarian cancer. Using a coculture assay system, the capacity of ovarian cancer cells to migrate through the mesothelium varied among ovarian cancer cell lines, showing a direct correlation with their ability to form tumors in immune compromised mice. Inhibition of the function of VCAM-1 or its ligand  $\alpha_4\beta_1$  integrin reduced, but did not completely inhibit, mesothelial invasion in this model system. Lastly, using a mouse metastatic ovarian cancer model, we show that treatment with function-blocking VCAM-1 antibodies increased survival and decreased tumor burden. Importantly, the majority of tumors in the treated mice were not invasive, correlating with the findings in the coculture system. These observations provide proof-of-principle evidence supporting VCAM-1 as a regulator of one aspect of ovarian cancer metastasis, that is, mesothelial invasion.

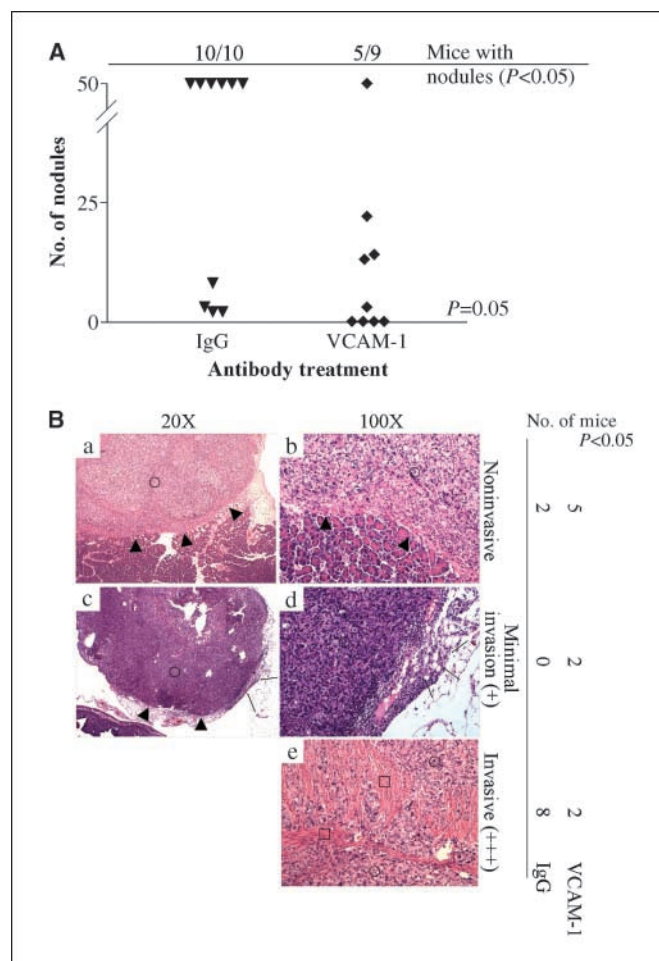


**Figure 6.** Anti-VCAM-1 antibody treatment delayed tumor formation and decreased tumor invasion in the orthotopic mouse model. **A**, the incidence of macroscopic tumor nodules was determined 4 wk after tumor initiation (above graph).  $\chi^2$  Test determined significance. The number of nodules per mouse is plotted. Mice with too many nodules to count were assigned a value of 50. Mann-Whitney statistic determined significance. **B**, the extent of tumor invasion was evaluated 4 wk after tumor initiation on H&E-stained tumor sections. Representative low-power ( $\times 20$ ) and high-power ( $\times 100$ ) images are depicted. Examples of noninvasive (**a** and **b**), minimally invasive (**c** and **d**), and highly invasive (**e**) tumors are shown. Arrowheads point to the smooth interface between the tumor (*open circle*) and underlying tissue (*open squares*). Arrows, a small region of tumor infiltration. **a** to **d**, two individual anti-VCAM-1-treated mice; **e**, control animal. The number of IgG or anti-VCAM-1-treated mice with noninvasive, minimally invasive, or invasive tumor nodules is enumerated to the right.  $\chi^2$  Test identified significance.



VCAM-1 mRNA is present within the mesothelium of microdissected peritoneal biopsies of women with ovarian cancer (10). The data presented here confirm a statistically significant difference in VCAM-1 protein expression on the surface of mesothelial cells from patients with ovarian cancer compared with cancer-free women. Whereas the mechanisms that regulate VCAM-1 expression in ovarian cancer patients are unknown, a known inducer of VCAM-1 expression, TNF $\alpha$ , is expressed by ovarian cancer cells (25) and found in malignant ascites (26). However, VCAM-1 expression was observed in patients without evidence of peritoneal metastasis (i.e., stage I or II ovarian cancer) and in regions lacking ovarian cancer. Macrophages, which promote ovarian cancer metastasis (27), provide an additional source of TNF $\alpha$ . One possibility is that infiltrating or activated resident macrophages secrete TNF $\alpha$ , thus promoting ovarian cancer peritoneal invasion.

Ovarian cancer is known to metastasize by attaching to, and invading through, the mesothelium. An assay system described herein attempts to model aspects of the metastatic process. Ovarian cancer cells plated on mesothelial monolayers migrated to the underside of the monolayer, presumably by passing between adjoining cells as previously described (9, 28). An alternative possibility is that the cancer cells pass through individual mesothelial cells, as has been described for leukocyte extravasation (29). Several observations indicate that ovarian cancer cells cannot penetrate the monolayer simply by passing through preformed openings. Transmesothelial migration was reduced when the monolayer was fixed. Moreover, increasing monolayer permeability had no effect on transmesothelial migration. The ability of ovarian cancer cells to migrate through mesothelial monolayers in culture correlated with their ability to form invasive tumors in an orthotopic xenograft mouse model (20). SKOV-3 and ES-2 cells were the most proficient at transmesothelial migration and readily formed invasive tumors in immune compromised mice (20). On the other hand, OVCAR-3 cells passed inefficiently through the monolayer and did not form tumors (20). Thus, the coculture assay system mimics the invasive capability of ovarian cancer cells *in vivo* and supports the use of this model to study mechanisms that regulate invasion.

The observation that VCAM-1 was expressed preferentially on the mesothelium of ovarian cancer patients together with its known role in regulating leukocyte extravasation indicated that it might be a regulator of ovarian cancer cell invasion of the mesothelium. Indeed, the data presented here implicated VCAM-1 and  $\alpha_4\beta_1$  integrin as one but not the only regulator of ovarian cancer invasion of the mesothelium in cell culture. VCAM-1 regulates extravasation upon binding  $\alpha_4\beta_1$  or  $\alpha_9\beta_1$  integrins (11, 12), both of which were expressed on ovarian cancer cells. Function-blocking antibodies directed against VCAM-1 or  $\alpha_4\beta_1$  integrin subunits decreased transmesothelial migration, whereas antibodies directed against  $\alpha_9\beta_1$  or  $\alpha_5$  integrin, which does not interact with VCAM-1, had no effect. The extent of transmesothelial migration achieved by each ovarian cancer cell line correlated with the level of  $\alpha_4$  integrin expression, further implicating  $\alpha_4\beta_1$  integrin in this process. These observations were supported by siRNA knockdown studies. Knockdown of VCAM-1 or  $\alpha_4$  integrin decreased transmesothelial migration by 50%. Importantly,  $\alpha_4$  integrin knockdown had no effect on ovarian cancer cell migration (data not shown), indicating that the knockdown targeted a specific component of the cooperation between ovarian cancer and mesothelial cells rather than simply inhibited ovarian cancer cell function.

The identification of VCAM-1 and  $\alpha_4\beta_1$  integrin as regulators of transmesothelial migration led to the hypothesis that these molecules might regulate ovarian cancer metastasis *in vivo*, which was tested in a mouse model. I.p. injection of ovarian cancer cells into immune compromised mice resulted in elevated VCAM-1 expression on the mesothelium within 2 weeks and the formation of ovarian cancer tumor nodules throughout the peritoneal cavity within 4 weeks of injection. By 6 weeks, extensive carcinomatosis was observed in addition to accumulation of ascites and the presence of micrometastases within the lungs. It is important to note that parenchymal lung metastases are rarely observed in human ovarian cancer; however, current imaging modalities are unable to detect microscopic lesions, which were observed in the mouse model. Although women with ovarian cancer succumb to extensive abdominal tumor bulk, it is possible that they contain lung metastases below the level of detection; microscopic examination of lungs from these women has not been reported.

We provide evidence showing that inhibition of VCAM-1 delayed but did not completely inhibit ovarian cancer metastatic progression. Treatment of tumor-bearing mice with function-blocking antibodies directed against VCAM-1 increased median survival by 30% and decreased tumor burden. The increased survival was associated with delayed appearance of macroscopic tumors, ascites, and microscopic lung metastases. Furthermore, anti-VCAM-1 antibody treatment reduced mesothelial invasion, corroborating the data obtained in the coculture model. One possibility is that functional blockade of VCAM-1 inhibits adhesion of ovarian cancer cells to the mesothelium, thus preventing establishment of tumors. However, VCAM-1 blocking antibodies had no effect on the ability of cancer cells to attach to mesothelial monolayers in culture (data not shown), and all anti-VCAM-1-treated mice had peritoneal tumors, which were primarily noninvasive. Because the blocking antibodies used in this study bind to the region of VCAM-1 that interacts with  $\alpha_4\beta_1$  integrin, and VCAM-1 blockade inhibited mesothelial invasion both in culture and *in vivo*, a more likely possibility is that VCAM-1 blockade prevents the establishment of metastases by limiting tumor cell access to growth-promoting factors within the underlying tissue and/or lymphovascular space (10). Indeed, human tumors that invade the mesothelium are more aggressive and associated with a less favorable prognosis than those growing on the mesothelium (30). The ability of VCAM-1 functional blockade to prevent mesothelial invasion and improve disease course in the mouse model strongly implicates VCAM-1 and its ligand  $\alpha_4\beta_1$  integrin in the regulation of ovarian cancer metastatic invasion and offers the exciting possibility of targeting VCAM-1- $\alpha_4\beta_1$  integrin interactions in the treatment of ovarian cancer.

## Disclosure of Potential Conflicts of Interest

R.L. Horst: President and Chief Executive Officer, Heartland Assays, Inc.; B.W. Hollis: Consultant, DiaSorin Corp., which conducted the assays for this analysis.

## Acknowledgments

Received 7/11/2008; revised 11/5/2008; accepted 12/10/2008; published OnlineFirst 02/10/2009.

**Grant support:** UVA Cancer Center, UVA Women's Oncology Research Fund, ACS Institutional Research Grant, Ovarian Cancer Research Fund, National Ovarian Cancer Coalition-Northern Virginia Division, and Marsha Rivkin Center for Ovarian Cancer Research (J.K. Slack-Davis).

The costs of publication of this article were defrayed in part by the payment of page charges. This article must therefore be hereby marked *advertisement* in accordance with 18 U.S.C. Section 1734 solely to indicate this fact.

We thank Lisa Vohwinkel for technical assistance and the Women's Oncology and Breast Cancer Research Groups for helpful comments and suggestions. J.K. Slack-Davis thanks J.T. Parsons for mentorship and support.

## References

1. Jemal A, Siegel R, Ward E, et al. Cancer statistics, 2008. *CA Cancer J Clin* 2008;58:71–96.
2. Ozols RF. Treatment goals in ovarian cancer. *Int J Gynecol Cancer* 2005;15 Suppl 1:3–11.
3. Agarwal R, Kaye SB. Ovarian cancer: strategies for overcoming resistance to chemotherapy. *Nat Rev Cancer* 2003;3:502–16.
4. Bell DA, Longacre TA, Prat J, et al. Serous borderline (low malignant potential, atypical proliferative) ovarian tumors: workshop perspectives. *Human Pathology* 2004;35:934–48.
5. Rieppi M, Vergani V, Gatto C, et al. Mesothelial cells induce the motility of human ovarian carcinoma cells. *Int J Cancer* 1999;80:303–7.
6. Ren J, Xiao Y-j, Singh LS, et al. Lysophosphatidic acid is constitutively produced by human peritoneal mesothelial cells and enhances adhesion, migration, and invasion of ovarian cancer cells. *Cancer Res* 2006;66:3006–14.
7. Xu Y, Gaudette DC, Boynton JD, et al. Characterization of an ovarian cancer activating factor in ascites from ovarian cancer patients. *Clin Cancer Res* 1995;1:1223–32.
8. Lessan K, Aguiar DJ, Oegema T, Siebenson L, Skubitz AP. CD44 and  $\beta$  integrin mediate ovarian carcinoma cell adhesion to peritoneal mesothelial cells. *Am J Pathol* 1999;154:1525–37.
9. Niedbala MJ, Crickard K, Bernacki RJ. Interactions of human ovarian tumor cells with human mesothelial cells grown on extracellular matrix. An *in vitro* model system for studying tumor cell adhesion and invasion. *Exp Cell Res* 1985;160:499–513.
10. Wang E, Ngalame Y, Panelli MC, et al. Peritoneal and subperitoneal stroma may facilitate regional spread of ovarian cancer. *Clin Cancer Res* 2005;11:113–22.
11. van Buul JD, Hordijk PL. Signaling in leukocyte transendothelial migration. *Arterioscler Thromb Vasc Biol* 2004;24:824–33.
12. Cannistra SA, Ottensmeier C, Tidy J, DeFranzo B. Vascular cell adhesion molecule-1 expressed by peritoneal mesothelium partly mediates the binding of activated human T lymphocytes. *Exp Hematol* 1994;22:996–1002.
13. Tomita Y, Saito T, Saito K, Oite T, Shimizu F, Sato S. Possible significance of VLA-4 ( $\alpha_4\beta_1$ ) for hematogenous metastasis of renal-cell cancer. *Int J Cancer* 1995;60:753–8.
14. Prifti S, Zourab Y, Koumouridis A, Bohlmann M, Strowitzki T, Rabe T. Role of integrins in invasion of endometrial cancer cell lines. *Gynecol Oncol* 2002;84:12–20.
15. Cannistra SA, Ottensmeier C, Niloff J, Orta B, DiCarlo J. Expression and function of  $\beta_1$  and  $\alpha_v\beta_3$  integrins in ovarian cancer. *Gynecol Oncol* 1995;58:216–25.
16. Wu L, Bernard-Trifilo JA, Lim Y, et al. Distinct FAK-Src activation events promote  $\alpha_5\beta_1$  and  $\alpha_4\beta_1$  integrin-stimulated neuroblastoma cell motility. *Oncogene* 2008;27:1439–48.
17. Schadendorf D, Gawlik C, Haney U, Ostmeier H, Suter L, Czarnetzki BM. Tumour progression and metastatic behaviour *in vivo* correlates with integrin expression on melanocytic tumours. *J Pathol* 1993;170:429–34.
18. Okahara H, Yagita H, Miyake K, Okumura K. Involvement of very late activation antigen 4 (VLA-4) and vascular cell adhesion molecule 1 (VCAM-1) in tumor necrosis factor  $\alpha$  enhancement of experimental metastasis. *Cancer Res* 1994;54:3233–6.
19. Garofalo A, Chirivi RGS, Foglieni C, et al. Involvement of the very late antigen 4 integrin on melanoma in interleukin 1-augmented experimental metastases. *Cancer Res* 1995;55:414–9.
20. Shaw TJ, Senterman MK, Dawson K, Crane CA, Vanderhyden BC. Characterization of intraperitoneal, and metastatic xenograft models of human ovarian cancer. *Mol Ther* 2004;10:1032–42.
21. Miyake K, Medina K, Ishihara K, Kimoto M, Auerbach R, Kincade PW. A VCAM-like adhesion molecule on murine bone marrow stromal cells mediates binding of lymphocyte precursors in culture. *J Cell Biol* 1991;114:557–65.
22. Stockton RA, Schaefer E, Schwartz MA. p21-activated kinase regulates endothelial permeability through modulation of contractility. *J Biol Chem* 2004;279:46621–30.
23. Calzada MJ, Zhou L, Sipes JM, et al.  $\alpha_4\beta_1$  Integrin mediates selective endothelial cell responses to thrombospondins 1 and 2 *in vitro* and modulates angiogenesis *in vivo*. *Circ Res* 2004;94:462–70.
24. Halder J, Kamat AA, Landen CN, Jr., et al. Focal adhesion kinase targeting using *in vivo* short interfering RNA delivery in neutral liposomes for ovarian carcinoma therapy. *Clin Cancer Res* 2006;12:4916–24.
25. Szlosarek PW, Grimshaw MJ, Kulbe H, et al. Expression and regulation of tumor necrosis factor  $\alpha$  in normal and malignant ovarian epithelium. *Mol Cancer Ther* 2006;5:382–90.
26. Moradi MM, Carson LF, Weinberg B, Haney AF, Twigg LB, Ramakrishnan S. Serum and ascitic fluid levels of interleukin-1, interleukin-6, and tumor necrosis factor  $\alpha$  in patients with ovarian epithelial cancer. *Cancer* 1993;72:2433–40.
27. Robinson-Smith TM, Isaacsohn I, Mercer CA, et al. Macrophages mediate inflammation-enhanced metastasis of ovarian tumors in mice. *Cancer Res* 2007;67:5708–16.
28. Sawada M, Shii J, Akedo H, Tanizawa O. An experimental model for ovarian tumor invasion of cultured mesothelial cell monolayer. *Lab Invest* 1994;70:333–8.
29. Carman CV, Springer TA. Trans-cellular migration: cell-cell contacts get intimate. *Curr Opin Cell Biol* 2008;20:533–40.
30. Hart WR. Borderline epithelial tumors of the ovary. *Mod Pathol* 2005;18 Suppl 2:S33–50.



# Cancer Research

The Journal of Cancer Research (1916–1930) | The American Journal of Cancer (1931–1940)

## Vascular Cell Adhesion Molecule-1 Is a Regulator of Ovarian Cancer Peritoneal Metastasis

Jill K. Slack-Davis, Kristen A. Atkins, Christine Harrer, et al.

*Cancer Res* Published OnlineFirst February 10, 2009.

<b>Updated version</b>	Access the most recent version of this article at: doi: <a href="https://doi.org/10.1158/0008-5472.CAN-08-2678">10.1158/0008-5472.CAN-08-2678</a>
<b>Supplementary Material</b>	Access the most recent supplemental material at: <a href="http://cancerres.aacrjournals.org/content/suppl/2009/02/09/0008-5472.CAN-08-2678.DC1">http://cancerres.aacrjournals.org/content/suppl/2009/02/09/0008-5472.CAN-08-2678.DC1</a>

<b>E-mail alerts</b>	<a href="#">Sign up to receive free email-alerts</a> related to this article or journal.
----------------------	--

<b>Reprints and Subscriptions</b>	To order reprints of this article or to subscribe to the journal, contact the AACR Publications Department at <a href="mailto:pubs@aacr.org">pubs@aacr.org</a> .
-----------------------------------	--

<b>Permissions</b>	To request permission to re-use all or part of this article, contact the AACR Publications Department at <a href="mailto:permissions@aacr.org">permissions@aacr.org</a> .
--------------------	---